Waste-to-Hydrogen pathways: Gas composition and char structure evolution during pyrolysis of food and digestate waste

International Journal of Hydrogen Energy 218 (2026) 153906

Contents lists available at ScienceDirect

International Journal of Hydrogen Energy

journal homepage: www.elsevier.com/locate/he

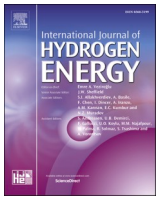

Waste-to-Hydrogen pathways: Gas composition and char structure evolution during pyrolysis of food and digestate waste

Davide Papurello [a,b,*], Kutlu Somek [a,c], Yeshui Zhang [d], Davide Dionisi [d], Tian Heng Qin [d], Tian Wang [d], Andrea Lanzini [a,b]

[a] Department of Energy, Politecnico di Torino, Corso Duca degli Abruzzi, 24, Turin, Italy
[b] Energy Center, Politecnico di Torino, Via Paolo Borsellino 38/16, 10138, Turin, Italy
[c] Faculty of Chemical and Metallurgical Engineering, Chemical Engineering Department, Yildiz Technical University, Davutpasa Street No.127, Esenler, 34220, Istanbul, Türkiye
[d] School of Engineering, University of Aberdeen, Aberdeen, AB24 3UE, UK

ARTICLE INFO

Keywords:
Hydrogen
Biochar
Carbon
Food waste
Digestate
Pyrolysis

ABSTRACT

This study investigates the influence of pyrolysis temperature on the yield distribution and gas composition of biochars derived from food waste (FW) and digestate waste (DW). Pyrolysis experiments were performed at 400–700 °C, and the resulting solid, liquid, and gas fractions were characterised. Gas compositions were quantified using Gas Chromatography (GC), while structural and physicochemical properties of the biochars were evaluated using SEM-EDS, BET, XRD, Raman spectroscopy, and TPO-DTG analysis. The proportion of syngas components, particularly hydrogen (H_2), showed a pronounced dependence on temperature and feedstock type. No detectable H_2 was found at 400 °C for either feedstock, whereas a substantial increase occurred with temperature elevation. For FW-derived gas, H_2 increased from 7.41 vol% at 500 °C to 26.57 vol% at 700 °C. Similarly, DW-based gas exhibited an increase from 6.68 vol% to 18.28 vol% across the same temperature range. This rise was accompanied by a reduction in CO_2 and an increase in CH_4 and light hydrocarbons. Raman spectroscopy revealed a temperature-dependent structural transition, indicated by increasing ID/IG ratios from 0.57 to 0.76 in FW biochar and 0.59 to 0.67 in DW biochar, confirming enhanced disorder and defect formation, particularly in FW. Overall, the thermochemical evolution of both feedstocks demonstrates that increasing pyrolysis temperature significantly enhances hydrogen generation capacity, most notably in food waste, where H_2 production increased from undetectable levels at 400 °C to 26.57 vol% at 700 °C, underscoring the strong potential of temperature-driven pathways for producing hydrogen-rich syngas from waste materials.

1. Introduction

The increasing rate of urbanisation has raised growing concerns about the management and valorisation of food waste and wastewater. Globally, food waste generation is estimated at around 1.3 billion tons, while sewage sludge production ranges between 75 and 100 million tons, and both are projected to increase further with ongoing urban expansion [1,2]. The production of high-value-added materials from these wastes has become a key focus area for both waste management operators and policymakers. Beyond thermochemical routes, waste management and valorisation can also be achieved through biological and chemical treatment technologies. Biological processes such as anaerobic digestion and composting are widely applied for organic waste stabilisation and energy recovery, with anaerobic digestion enabling biogas production under mild operating conditions, albeit with limited hydrogen yield and strong sensitivity to feedstock composition and process stability [3–5]. Chemical treatment routes, including hydrolysis, chemical extraction, and wet oxidation, have been explored for nutrient recovery, organic matter solubilisation, and pre-treatment prior to energy conversion, but they often require chemical reagents and generate secondary waste streams that must be further managed [6,7]. Compared to these approaches, thermochemical processes—particularly pyrolysis and gasification—offer greater flexibility in handling heterogeneous waste streams and enable simultaneous production of energy-rich gases and stable carbonaceous solids, making them attractive for integrated waste-to-energy and material valorisation strategies

* Corresponding author. Department of Energy, Politecnico di Torino, Corso Duca degli Abruzzi, 24, Turin, Italy.
E-mail address: davide.papurello@polito.it (D. Papurello).

https://doi.org/10.1016/j.ijhydene.2026.153906
Received 5 December 2025; Received in revised form 3 February 2026; Accepted 4 February 2026
Available online 14 February 2026

[8,9]. Thanks to their high organic content, food waste (FW) and wastewater treatment sludge (WWT) are promising raw materials for thermochemical conversion processes. Using these materials for hydrogen synthesis, energy recovery and carbon-rich char production not only reduces the overall waste volume but also provides an effective route for the recovery of metals, minerals, and phosphorus, particularly from WWT sludges [10]. As highlighted in the Global Hydrogen Review, global hydrogen production was around 97 million tonnes in 2023, and fossil resources remain the dominant production route. The transition to hydrogen production from waste streams offers a combined environmental benefit: it reduces the impact of municipal and industrial waste while also lowering CO_2 emissions, as hydrogen combustion produces no direct carbon emissions and can replace fossil fuel energy carriers [11]. This approach not only mitigates the release of potentially harmful elements into the environment but also supports circular resource utilisation and sustainable waste management, while simultaneously enabling low-carbon hydrogen production. On the other hand, biochar, one of the main products of the pyrolysis process, has a wide range of applications, particularly in energy systems, composite material development, pollutant remediation, medical applications and soil improvement [4,12–14]. All these applications highlight the importance of hydrogen and other pyrolysis production and synthesis methods from a sustainability perspective. Hydrogen and char synthesis can be produced through various thermochemical conversion methods, among which pyrolysis, HydroThermal Carbonisation (HTC), gasification, and torrefaction are the most widely investigated. Pyrolysis is a thermochemical conversion process in which organic materials are heated in an oxygen-free environment, resulting—through a complex network of primary and secondary reactions—in the formation of three main product fractions: a solid carbon-rich residue (char), a condensable liquid phase (bio-oil/tar), and a permanent gaseous fraction. Depending on the targeted product, different pyrolysis regimes can be employed, commonly classified as slow, fast, and flash pyrolysis, which differ primarily in heating rate and residence time. Slow pyrolysis, characterised by low heating rates and long residence times, typically favours higher solid (char) yields, lower liquid yields, and enhanced gas formation, whereas fast and flash pyrolysis are generally designed to maximise liquid production. In the present study, the operating conditions adopted correspond to a slow pyrolysis regime, consistent with the dual objective of char production and syngas characterisation. The HydroThermal Carbonisation (HTC) process, relies on the carbonisation of biomass in the presence of water under high-temperature and pressure conditions. Gasification is a high-temperature process conducted in a limited oxygen or steam atmosphere to generate synthesis gas (syngas), typically characterised by low char yield [9]. Torrefaction is carried out at low temperatures and atmospheric pressure and is considered a pre-treatment process aimed at improving the combustible properties of biomass [15]. When these methods are evaluated collectively, pyrolysis stands out for its ability to generate hydrogen and other energy-rich gaseous products, while simultaneously producing carbon-rich charcoal with a porous structure, large surface area and strong carbon stability [8,16,17]. Furthermore, pyrolysis offers substantial benefits beyond the production of hydrogen and energy-rich gases, including the generation of biochar suitable for applications in composite materials and a wide range of other high-value uses [18]. However, it is important to clearly recognise that pyrolysis is not intrinsically a hydrogen-maximising process and should not be considered a standalone hydrogen production route when compared with gasification or catalytic reforming technologies. In this context, pyrolysis should be regarded not as a hydrogen-maximising technology, but rather as a syngas-forming and feedstock-conditioning step within a broader waste-to-hydrogen framework. The process inherently produces a hydrogen-rich syngas in which H_2 is accompanied by CO, CH_4 and light hydrocarbons, with their relative proportions governed by temperature and feedstock composition. By contrast, thermochemical routes such as biomass gasification and catalytic reforming are specifically designed to maximise hydrogen yield through steam-assisted reactions and equilibrium-shifting mechanisms, achieving substantially higher hydrogen recovery efficiencies [19–21].

Early comparative work on food-waste pyrolysis and gasification established that gas composition and hydrogen yield are strongly temperature-dependent and that the overall hydrogen potential must be evaluated alongside total gas production rather than using H_2 vol% alone [22]. More recent FW-focused strategies have explored integrated configurations (e.g., in situ gasification after pyrolysis) specifically to increase hydrogen-rich syngas quality and process efficiencies [23]. In parallel, a substantial body of literature has addressed FW-derived biochar production and optimisation, emphasising that pyrolysis conditions (temperature, additives/catalysts) govern aromaticity, surface area, ash/mineral retention and potential end uses. A dedicated review on converting food waste into biochars highlights the importance of feedstock heterogeneity and operating severity in determining char yield and properties, and points to the need for consistent, comparable performance metrics across studies [24]. A recent FW biochar study further demonstrates how formulation and catalytic additives can be used to tailor char and co-products, supporting the relevance of systematic char characterisation when evaluating FW pyrolysis pathways [25]. For digestate and digestate-derived residues, pyrolysis has been extensively explored because high ash/mineral fractions and nutrient-rich matrices strongly affect char yield, stability and surface development. Systematic studies on digestate pyrolysis show that temperature governs devolatilization [26] and char structural evolution, while minerals can stabilise the carbon matrix and influence porosity development [26]. Recent experimental work on sewage sludge pyrolysis reports hydrogen-rich syngas generation and optimisation using statistical approaches [27], while two-stage concepts that couple pyrolysis with catalytic conversion explicitly demonstrate the role of downstream upgrading in boosting hydrogen production [28].

Despite the extensive literature on food waste and digestate pyrolysis, several gaps remain. Most studies examine the two feedstocks separately and under different operating conditions, limiting direct comparison of their thermochemical behaviour. In addition, hydrogen production is often reported only as volumetric concentration rather than normalised yield, and gas composition and char properties are rarely discussed in an integrated manner. As a result, the influence of feedstock composition and mineral content on the trade-off between hydrogen-rich syngas formation and char stability is still not fully understood. To address these limitations, the present study investigates hydrogen and char production from two representative waste streams—food waste (FW) and digestate waste (DW)—using a bed reactor under identical pyrolysis conditions between 400 and 700 °C, with nitrogen as an inert carrier gas. To evaluate the potential of hydrogen production capacity, applications of the obtained char, detailed structural and morphological characterisations were performed using Scanning Electron Microscopy coupled with Energy Dispersive Spectroscopy (SEM-EDS), Temperature-Programmed Oxidation and Derivative Thermogravimetry (TPO-DTG), Gas Chromatography (GC), X-Ray Diffraction (XRD), Brunauer–Emmett–Teller (BET) and Raman spectroscopy analyses. Furthermore, the variations in the compositions of CH_4, CO, and CO_2 gases with temperature were examined, and the potential utilisation of these by-products was discussed. Nevertheless, the lack of detailed insight into the coupled optimisation of hydrogen synthesis, char valorisation, and gaseous by-product utilisation from mixed municipal waste sources represents a major research gap that this study directly investigates.

2. Materials and methods

2.1. Biomass waste material preparation

The Food Waste (FW) and Digestate Waste (DW) samples used in this study were collected from the central water treatment plant of the city of

Aberdeen (Nigg Wastewater treatment plant in Aberdeen, Scotland) and the plant that treats organic waste (John Rennie & Sons, Gask Farm, Turriff, Aberdeenshire, Scotland, AB53 8BP). The samples were subjected to a pre-treatment process involving pre-drying at 105 °C (± 5 °C), using an electric oven (Memmert UM200, Germany) for 24 h to remove moisture, after which they were prepared for use in the pyrolysis reactor.

2.2. Pyrolysis reactor and methodology

The char production process was carried out using a bed pyrolysis reactor (24 mm inner diameter, 1000 mm long), as illustrated in Fig. 1 and used in a previous work [29]. The temperature and reaction duration were controlled through a Multi Position Tube Furnace (Elite Thermal Systems Ltd, 6 Stuart Rd, Market Harborough LE16 9PQ, UK), while a continuous flow of nitrogen gas (40 mL min^{-1}, at standard conditions) was supplied via the control panel to maintain an oxygen-free atmosphere during the pyrolysis process.

The synthesis experiments were conducted at 400, 500, 600, and 700 °C under controlled operating conditions. During all experiments, the samples were heated to the target temperatures at a heating rate of 20 °C min^{-1} and maintained for 1 h to complete the pyrolysis process. The residence time chosen at the target temperature was chosen to ensure complete devolatilization and stabilisation of both the gas and char phases. The heating rate chosen represents a compromise between laboratory-scale slow pyrolysis conditions and industrially relevant thermal ramps and was selected to limit internal temperature gradients while still promoting secondary cracking reactions at higher temperatures. The nitrogen flow rate (40 mL min^{-1}) was selected to maintain an inert atmosphere and ensure efficient removal of volatile products, while minimising dilution effects on gas composition analysis. A cold trap was used to retain the liquid fraction. At the end of the test, the char was removed from the tubular reactor, weighed (DEAdventurer Pro AV4102C) and sieved. In the following table, Table 1 The solid samples in the reactor before and after the pyrolysis reaction are shown.

The samples produced was then ground and sieved to a size between 50 and 180 μm.

2.3. Characterisation and analysis procedure

Structural characterisation was performed using a Renishaw in Via Raman Microscope, with Leica Microsystems DM2700 M Ren RL/TL, using 514 nm laser (RL515-08) as excitation source. Raman spectrometer in the 1100–1700 cm^{-1} wavenumber range. Morphological analysis and elemental composition were determined using a ZEISS Gemini SEM 300 (SEM-EDS) instrument at magnifications ranging from 5k to 25k (Carl Zeiss Industrielle Messtechnik GmbH, Germany). Surface area and pore characterisation analysis was performed using a

Table 1
Solid phase of the samples before and after the pyrolysis reaction in the reactor.

Feedstock	T (°C)	Solid phase	
		Before reaction (g)	After reaction (g)
FW	400	15.25	9.77
FW	500	15.51	8.15
FW	600	17.61	8.66
FW	700	17.06	7.32
DW	400	38.64	24.89
DW	500	33.13	17.81
DW	600	34.42	17.35
DW	700	41.05	18.79

Brunauer–Emmett–Teller (BET) surface area analyser. The porous properties of the catalysts were determined by obtaining the N_2 adsorption and desorption isotherms at equilibrium vapour pressure using the static volumetric method (ISO 9277 and ASTM D3663). N_2 adsorption–desorption isotherms were recorded at −196 °C using a TriStar II Plus instrument (Micromeritics). The samples were degassed at 300 °C for 4 h before analysis. Specific surface areas were determined according to the Brunauer, Emmett and Teller (BET) model, with pore diameters, volumes and size distributions determined through Barrett-Joyner-Halenda (BJH) desorption analysis. The chemical composition and crystalline structure of the samples were analysed using an XRD instrument. Room temperature ex-situ XRD data sets were obtained using a STOE Stadi-Powder X-ray diffractometer equipped with a Mo tube set to 55 kV and 40 mA (Kα1 with λ = 0.7093 Å), a primary beam monochromator and a Dectris Mythen detector. Measurements were performed in this capillary (0.5 mm) transmission mode with the 2θ range of 2° to 50°. The data was acquired using the STOE WinXPOW program (version 3.20). The samples were analysed by temperature programme oxidation (TPO) using a thermogravimetric analyser (TGA) (Mettler Toledo TGA/DSC 3 + system) to determine the oxidation characteristics of carbon on the samples (ASTM E1131). Each sample was placed in the TGA and heated in air at a flow rate of 20 mL min–1 to 900 °C at a heating rate of 15 °C min^{-1}. All samples were held at 120 °C for 10 min to remove moisture. The gaseous products were collected in Tedlar® sampling bags and analysed using a Trace 1300 gas chromatograph (Thermo Fisher Scientific) equipped with a thermal conductivity detector (TCD) and a capillary column (30 m × 0.25 mm, TraceGOLD™ TG-WaxMS A). Helium served as the carrier gas, with a column flow rate of 6.5 mL min^{-1} and a split flow of 65 mL min^{-1}. The inlet temperature was maintained at 150 °C. The oven temperature was held at 35 °C for 3 min, increased to 80 °C at 10 °C min^{-1}, then ramped to 250 °C at 30 °C min^{-1} and held for 10 min. The TCD temperature was set to 160 °C.

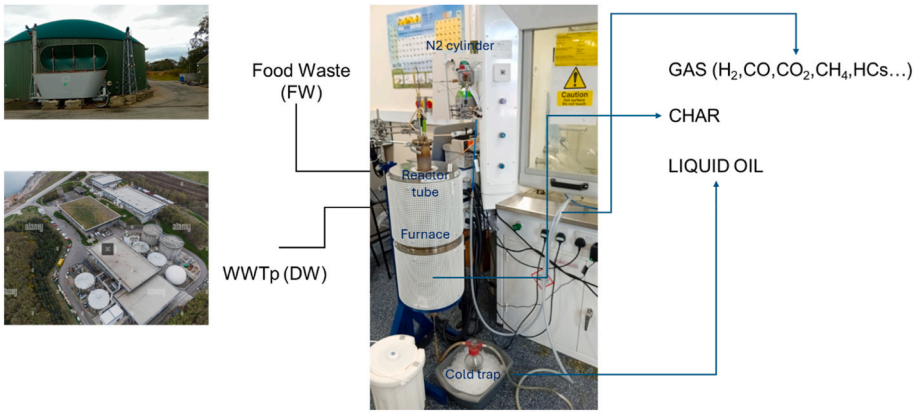

Fig. 1. Product transfer ratio of FW and DW biochars at temperatures between 400 and 700 °C.

3. Results and discussion

3.1. Product transition ratio of food waste and digestate waste yield

To determine the product distribution ratios, Equations (1)–(3) were applied. In this context, the initial feedstock mass is denoted as M, the mass of condensed products (tar and bio-oil) is represented as M_{tar}, and the gaseous product yield is expressed as P_{gas}.

$$Pchar = \frac{Mchar}{M} * 100 \quad (1)$$

$$Ptar = \frac{Mtar}{M} * 100 \quad (2)$$

$$Pgas = 100 - Ptar - Pchar \quad (3)$$

Fig. 2 shows the product yields, evaluated by mass, obtained from the pyrolysis of digestate and food waste in the temperature range of 400–700 °C. A decrease in char yield was observed for food and digestate waste with increasing temperature, which can be attributed to its high volatile matter content and the enhanced devolatilization at elevated temperatures. This trend is consistent with previously reported findings [30]. Overall, the results indicate that digestate is suitable for char-oriented applications, due to the higher char fraction achieved, whereas food waste shows potential for energy recovery, such as syngas production.

3.2. Hydrogen production efficiency of food waste and digestate waste at different pyrolysis temperatures

The volumetric composition of the pyrolysis gases (H_2, CO, CH_4, CO_2, C_2H_4, C_2H_6, C_3H_6, and C_3H_8) obtained from the process was determined via GC-TCD analysis, and the results are presented in Fig. 3(a and b) as well as in Tables S1 and S2. To ensure the reliability of both the hydrogen and other gases production procedure and GC-TCD measurements, each sample (FW and DW) was pyrolysed twice at each temperature, and all analyses were conducted using the replicated samples. Based on the results, Hydrogen gas was not detected at the lowest pyrolysis temperature in either sample type. However, its concentration increased proportionally with temperature. The average H_2 content reached 26.57% in FW700 and 18.28% in DW700 samples. These trends are consistent with previously reported findings in the literature [31,32].

In addition, hydrogen production can be further enhanced through steam reforming, which is a technically efficient and commercially established industrial process [33]. When applied to waste-derived syngas, the methane content, particularly at elevated pyrolysis temperature, offers a valuable opportunity to increase overall hydrogen yield and transform the system into a more efficient energy conversion pathway. The methane concentration exhibited a clear temperature-dependent trend, increasing steadily as the pyrolysis temperature rose for both feedstocks. At 400 °C, CH_4 levels remained relatively low, ranging between 4.87 and 5.06 vol% for FW and 13.42–13.44 vol% for DW. However, a pronounced increase was observed above 500 °C, indicating intensified secondary cracking and hydrocarbon reforming processes. The highest methane fractions were obtained at 700 °C, reaching 26.17 vol% for FW and 40.72 vol% for DW, demonstrating the strong influence of thermal severity on methane formation mechanisms. Examination of the H_2/CO ratios showed the highest values in FW700 and DW700 samples, with 2.17 and 1.78, respectively. Since the H_2/CO ratio plays a critical role in Fischer–Tropsch synthesis efficiency, the fact that FW700 exhibits a ratio ≥2 indicates a significant advantage and strong potential for syngas utilisation [34]. A decreasing trend was observed for CO_2 concentration with increasing temperature in both sample groups. The highest CO_2 content was detected in FW400 (83.27%) and DW400 (75.76%) samples [35]. Also, the highest methane concentration was measured in the DW700 sample, reaching 40.72%, while the maximum value for the FW700 sample was 26.17%. A similar trend was observed for the total hydrocarbon fraction (C_nH_m = C_2H_4, C_2H_6, C_3H_6, and C_3H_8), where FW700 exhibited 5.40% and DW700 showed 2.97%. Considering that higher hydrocarbon content contributes to an increased calorific value, the DW700 sample demonstrates a higher potential for energy recovery applications compared to the other samples [32,36].

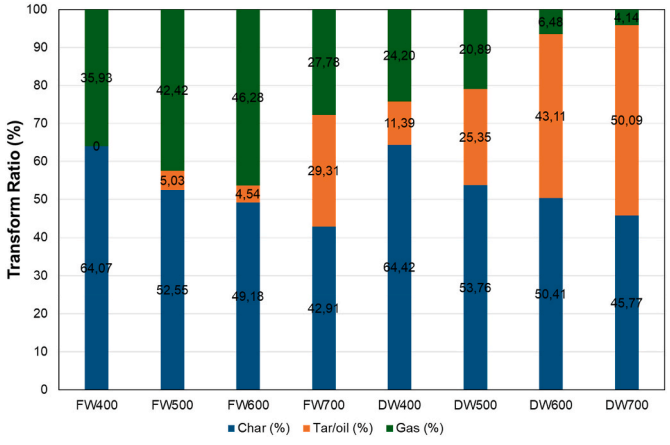

Fig. 2. Product transfer ratio of FW and DW biochars at temperatures between 400 and 700 °C.

The hydrogen yield normalised per kilogram of feedstock, and it was calculated starting from gas production (Fig. 1), passing through dry gas moles, calculating the total dry gas volume under normal conditions and calculating the hydrogen yield based on the information in Fig. 2. This table shows a clear dependence on both pyrolysis temperature and feedstock type (Table 2). For food waste (FW), no hydrogen is produced at 400 °C, while a measurable yield appears at 500 °C (0.020 Nm^3 H_2 kg^{-1}). The hydrogen yield reaches a maximum at 600 °C (0.078 Nm^3 H_2 kg^{-1}), resulting from the combined effect of a high gas yield and a substantial hydrogen fraction. Although the hydrogen concentration further increases at 700 °C, the total gas production decreases, leading to a slight reduction in hydrogen yield (0.073 Nm^3 H_2 kg^{-1}). Digestate waste (DW) exhibits significantly lower hydrogen yields across the entire temperature range. Hydrogen formation starts at 500 °C but remains limited (≈0.009 Nm^3 H_2 kg^{-1}) and further increases in hydrogen concentration at higher temperatures are offset by a sharp decline in total gas yield. As a result, the hydrogen yield remains nearly constant between 500 and 600 °C and decreases at 700 °C.

Overall, FW produces up to an order of magnitude more hydrogen per kilogram of feedstock than DW, particularly at 600–700 °C, confirming its greater suitability for waste-to-hydrogen pathways based on pyrolysis.

3.3. Thermal decomposition analysis of biochars

When the results presented in Fig. 4 are examined, it can be observed that the biochars obtained from both FW and DW samples exhibit stable structures at high temperatures. This finding is consistent with the literature and confirms similar results reported previously [37,38]. The accompanying DTG curves offer additional insight by identifying the temperatures at which the maximum mass-loss rates occur, thus revealing distinct decomposition stages and oxidative reactivity of the carbon matrix. DTG analysis is particularly valuable for distinguishing subtle structural transitions, identifying labile oxygen-containing functional groups, and quantifying char stability under oxidative conditions, making it a widely used technique in biochar research. For the samples obtained at 400 °C and 500 °C from FW and DW, decomposition becomes apparent around 300 °C, as indicated by the decrease observed. Moreover, the peak structure seen in the DTG curves within this

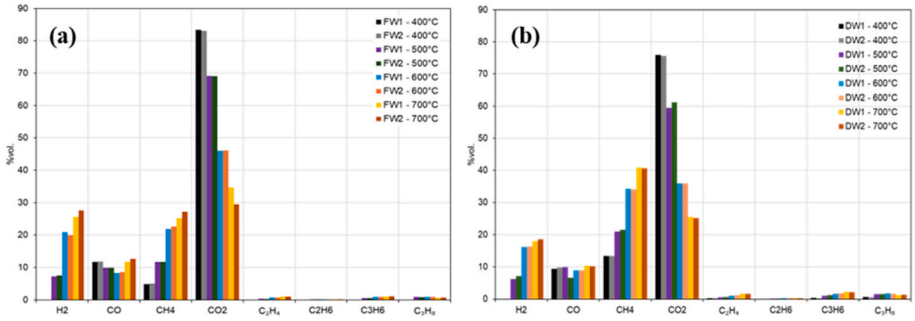

Fig. 3. Volume percentage composition of pyrolysis gases (GC-TCD) obtained from (a) FW1–FW2 and (b) DW1–DW2 biochars at temperatures between 400 and 700 °C.

Table 2
Hydrogen yield normalised per unit of feedstock ($Nm^3\ H_2\ kg^{-1}$) from food waste and digestate waste at different temperatures.

Feedstock	T (°C)	Gas yield (wt% of feed)	H_2 (vol %)	Total dry gas ($Nm^3\ kg^{-1}$)	H_2 yield ($Nm^3\ H_2\ kg^{-1}$)
FW	400	35.93	0.00	0.198	**0.0000**
FW	500	42.42	7.41	0.266	**0.0197**
FW	600	46.28	20.50	0.378	**0.0775**
FW	700	27.78	26.57	0.273	**0.0726**
DW	400	24.20	0.00	0.141	**0.0000**
DW	500	20.89	6.68	0.140	**0.00936**
DW	600	6.48	16.50	0.05696	**0.00940**
DW	700	4.14	18.28	0.0406	**0.00742**

temperature range further supports this observation. This behaviour suggests the presence of thermally labile functional groups (e.g., carboxyl, phenolic, and aliphatic moieties), which commonly persist in chars produced at mild pyrolysis temperatures. Similar oxidation behaviours have been observed in lignocellulosic- and sludge-derived chars with low aromaticity and higher oxygen content [38].

Biochars produced at 600 °C and 700 °C demonstrate markedly improved thermal stability, characterised by lower mass-loss rates and weaker DTG peak intensities. This reflects the formation of highly condensed aromatic domains and the progressive elimination of volatile compounds at higher pyrolysis temperatures. Notably, the DW700 sample exhibits the highest stability among all tested materials, which can be attributed to its elevated mineral content acting as a structural stabiliser. This behaviour aligns with earlier findings showing that ash components (e.g., Ca, Mg, Si, Fe minerals) can promote carbon matrix rigidity and suppress oxidative degradation [39].

Overall, the reduced DTG reactivity and diminished mass-loss rates at higher pyrolysis temperatures provide strong evidence for increased carbon condensation and enhanced intrinsic stability. These observations are consistent with previously published studies reporting that the degree of carbon ordering and aromatic clustering increases with temperature, resulting in biochars that resist thermal oxidation and exhibit higher long-term environmental stability [40].

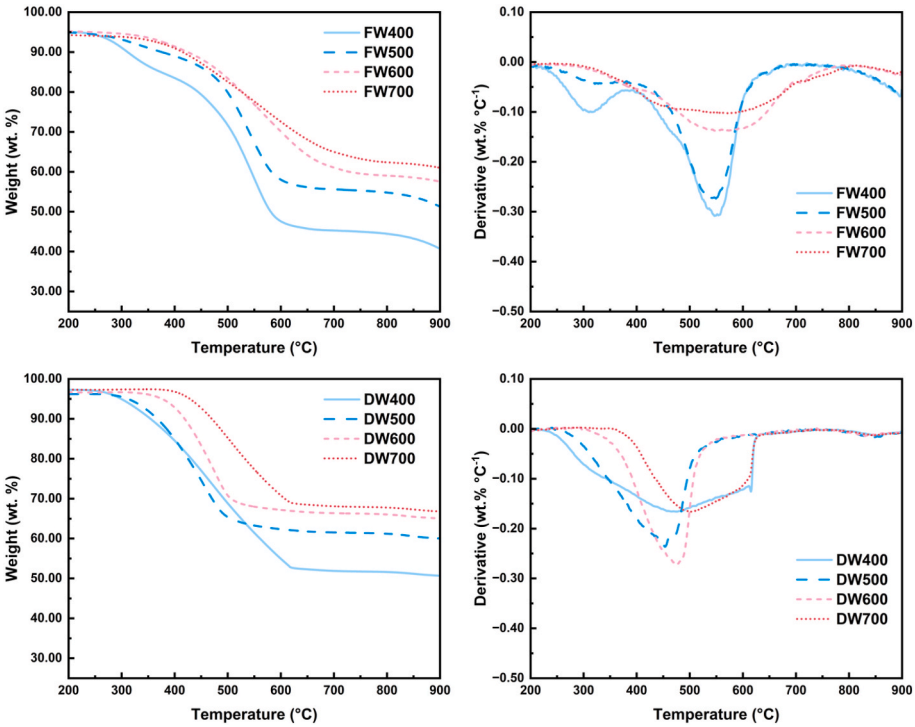

Fig. 4. Thermogravimetric (TGA) and derivative thermogravimetric (DTG) profiles of food waste (FW) and wastewater sludge (DW) biochars prepared at various pyrolysis temperatures.

3.4. Raman analysis of biochars

Raman spectroscopy is an analytical technique used to evaluate the degree of graphitic transformation in biochar samples and thereby assess the stability of their carbon structures. The defect (D) band appearing around ~1300 cm^{-1} and the graphitic (G) band near ~1600 cm^{-1} are analysed in Fig. 5, and the ratio of their intensities (I_D/I_G), as given in Table 3, is used to interpret the degree of disorder in the carbon structure of the biochar.

Raman spectroscopy results demonstrated that increasing pyrolysis temperature led to structural reorganisation in both food waste- and digestate-derived biochars. In the food waste biochars, the ID/IG ratio increased from 0.57 at 400 °C to 0.76 at 700 °C. This increase indicates that higher temperatures promote the development of aromatic carbon domains while simultaneously generating additional structural disorder, such as edge defects within the graphitic lattice. This trend is consistent with earlier studies, which report that under pyrolysis temperatures below 1000 °C, the release of volatile compounds enhances defect formation and structural disorder, reflected by the increase in ID/IG values [40,41]. In contrast, digestate-derived biochars exhibited a more moderate increase in ID/IG ratio, rising from 0.59 at 400 °C to 0.67 at 700 °C. This more limited change may be attributed to the higher ash and mineral content typically present in digestate biochar, which can contribute to a more thermally stable carbon framework and reduce the extent of defect development during thermal restructuring [39,42].

3.5. SEM analysis of biochars

The SEM analysis results, which were performed to evaluate the surface morphology and investigate the porosity as a key parameter for determining potential application areas of the char structures, are presented in Fig. 6 and Fig. S1–S8. Fig. 4 (1K magnification rate), together with the different (between 3K–25K) magnification rate SEM images presented in supported Fig. S1–S8, clearly demonstrates that the pyrolysis temperature exerts a strong influence on the surface morphology of both food waste (FW) and digestate (DW) biochars. At lower temperatures (400–500 °C), both materials exhibit compact and partially fused surfaces with limited pore development, indicating incomplete devolatilization. When the temperature increases to 600 °C, the FW samples develop a hierarchical and well-connected pore structure with thin walls and abundant micro- and mesopores, revealing extensive aromatisation and the formation of a stable carbon skeleton. Although DW samples also display increased porosity at this temperature, their high mineral and ash contents cause the accumulation of inorganic phases on the pore walls, which is observed as a white structural accumulation, partially blocking the structure. At 700 °C, FW largely retains its porous morphology with minor pore narrowing, whereas DW undergoes significant sintering and pore collapse due to the melting and redistribution of ash phases. These morphological transformations indicate that FW maintains a more thermally stable and continuous pore system, while DW deteriorates earlier because of its higher inorganic fraction. Comparison with previous studies confirmed that the obtained results are consistent with the literature data [40,43]. Overall, the optimal pyrolysis temperature for achieving maximum porosity and structural integrity is around 600 °C for FW and 500–600 °C for DW. Consequently, FW biochar—with its regular and interconnected pore network—is more suitable for adsorption and electrochemical applications, whereas DW biochar, due to its mineral-rich composition, is better suited for soil amendment or nutrient supplementation purposes [44,45]. On the other hand, qualitative EDS analysis indicates that Ba and S signals appear at higher intensities in the DW-derived char samples. This trend may be attributed to the presence of barium sulfate residues, potentially originating from chemicals used in wastewater treatment processes.

Table 3
Raman ID/IG ratios of Food Waste and Digestate Waste biochars produced at different pyrolysis temperatures.

	Food Waste (ID/IG)	Digestate Waste(ID/IG)
400°C	0.57	0.59
500°C	0.62	0.65
600°C	0.62	0.65
700°C	0.76	0.67

3.6. XRD results

XRD patterns of biochar samples derived from FW and DW within the temperature range of 400–700 °C are presented in Fig. 7. The results indicate that the most distinct diffraction peak in FW biochar appears at approximately 28.5°, corresponding to $CaCO_3$, whereas the dominant peak observed at 26.8° in DW samples is associated with silicon-based compounds. A peak detected at 31.5°, attributed to CaS, was found exclusively in FW samples with higher intensity. These observations are consistent with the SEM analyses. In addition, a diffraction peak at approximately 20.9° in DW biochar indicates the presence of crystalline cellulose, which was not observed in the FW samples. The peak identified near 40.6° corresponds to KCl, and its interpretation is supported by the elemental composition obtained from SEM–EDS analysis (Fig. S9–S12) and (Fig. S13–S16), where potassium was detected predominantly in FW samples. Weak peaks appearing in the 41–50° range are indicative of calcium- and silicon-containing phases. Overall, the observed diffraction behaviour aligns with previously reported studies [46,47]. Furthermore, peaks detected between 50 and 72° are attributed to silicate compounds containing Ca and Mg elements [47].

3.7. BET analysis

BET analysis results used to determine the specific surface area, pore volume, and pore diameter for both FW- and DW-derived biochars are presented in Table 4. The obtained data indicate that the pore structure evolution of the biochars strongly depends on pyrolysis temperature and differs significantly between the two feedstocks. In FW-derived biochars,

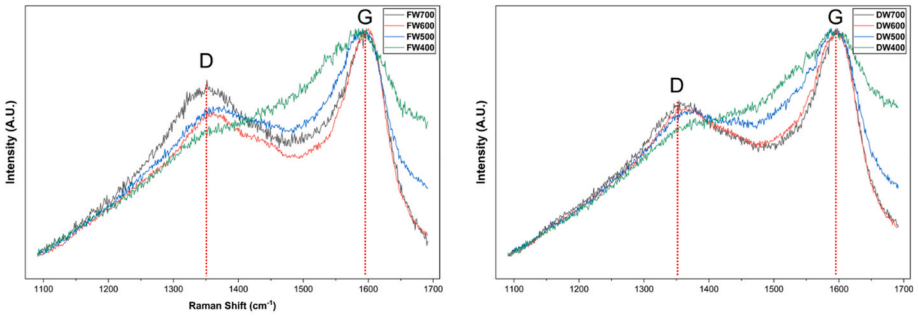

Fig. 5. Raman Spectrum of different pyrolysis temperatures (a)Food Waste (FW), and (b) Digestate Waste (DW).

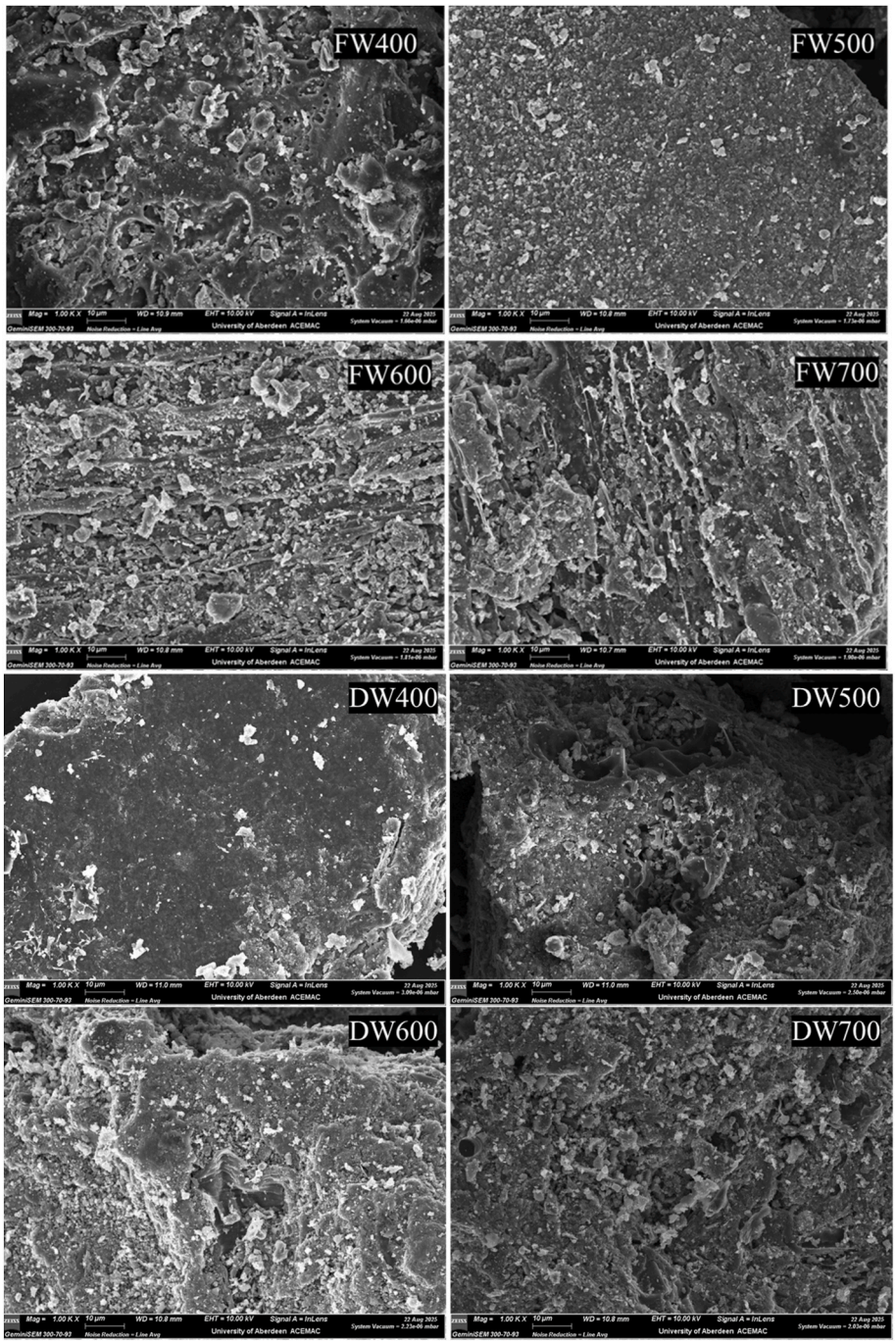

Fig. 6. SEM images of different pyrolysis temperatures of Food Waste (FW) and Digestate Waste (DW).

the specific surface area remained notably low at lower temperatures (400–600 °C) (0.34–6.62 m^2/g), and a meaningful development of porosity was observed only at 700 °C (38.37 m^2/g). This trend is consistent with literature reporting that the textural characteristics of food-waste biochar are highly sensitive to feedstock composition and thermal treatment conditions [48]. In contrast, DW-derived biochars exhibited earlier pore development, with the highest surface area achieved at 500 °C (75.30 m^2/g). The non-linear relationship between surface area and temperature can be attributed to pore expansion at elevated temperatures, where neighbouring pores merge and form larger but less surface-active structures. This behaviour aligns with previously reported mechanisms in digestate-derived biochar, where pore collapse, structural rearrangement, and mineral-assisted stabilisation may occur at higher temperatures. In addition, the structural patterns observed in Fig. S5–S8 further support this interpretation [49]. Overall, the results demonstrate that pyrolysis temperature and feedstock composition are key parameters governing the final surface area, pore volume, and microstructural properties of the produced biochars.

4. Conclusions and future works

This study demonstrates that pyrolysis temperature and feedstock characteristics exert a strong influence on gas composition and char properties derived from food waste (FW) and digestate waste (DW). Hydrogen formation shows a clear temperature dependence, increasing from undetectable levels at 400 °C to 26.57 vol% (0.0726 $Nm^3\ H_2\ kg^{-1}$ feedstock) for FW and 18.28 vol% (0.00742 $Nm^3\ H_2\ kg^{-1}$ feedstock) for DW at 700 °C. These results confirm that pyrolysis can effectively

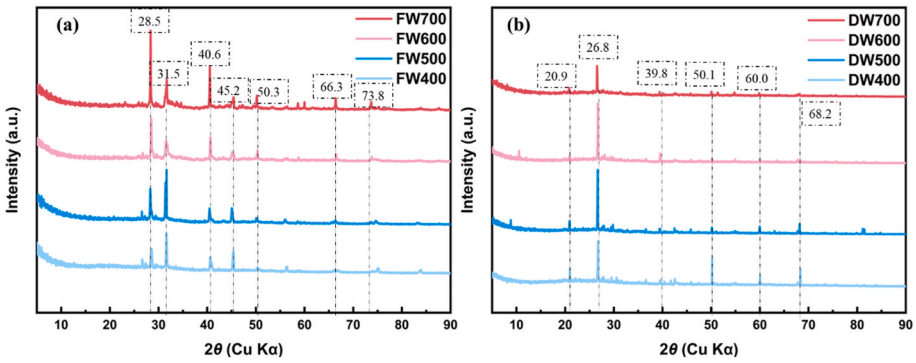

Fig. 7. XRD pattern of **(a)** FW and **(b)** DW biochars at temperatures between 400 and 700 °C.

Table 4
BET Surface area end pore characterisation analysis results of FW and DW biochars at temperatures between 400 and 700 °C.

Biochar Type	BET Surface Area (m^2g^{-1})	Total Pore Volume (cm^3g^{-1})	Mean Pore Diameter (nm)
FW400	0.34	0.011	129.41
FW500	6.62	0.019	11.48
FW600	3.20	0.011	13.75
FW700	38.37	0.033	3.44
DW400	11.86	0.085	28.67
DW500	75.30	0.136	7.22
DW600	35.86	0.118	13.16
DW700	44.09	0.134	12.16

generate hydrogen-rich syngas from waste streams, although it should be regarded as a syngas-forming and pre-conversion step rather than a hydrogen-maximising process. The comparative analysis highlights that FW exhibits a greater propensity for gas-phase conversion, yielding higher hydrogen quantities per unit of feedstock, whereas DW retains a larger solid fraction due to its higher ash and mineral content. Consequently, FW-derived char and gas products are more suitable for energy-oriented pathways, such as gasification or downstream syngas upgrading, while DW-derived char shows stronger potential for material and environmental applications, including soil amendment and nutrient recovery. The reduction in char yield with increasing temperature for FW reflects its higher volatile content, whereas the more stable char yields observed for DW are consistent with mineral-assisted structural stabilisation effects. Char characterisation results further support these trends. Raman spectroscopy indicates progressive carbon restructuring with increasing temperature in both feedstocks, with higher ID/IG ratios for FW suggesting greater defect formation and structural disorder compared to DW. SEM-EDS and BET analyses corroborate these observations, revealing more pronounced pore development and surface evolution in FW-derived chars, while mineral accumulation in DW chars contributes to enhanced thermal stability but reduced gas–solid interaction potential. In parallel, gas composition analysis shows that elevated temperatures improve syngas quality, with FW700 exhibiting the highest H_2/CO ratio and DW700 the highest methane concentration, pointing towards distinct upgrading and energy recovery routes for the two waste streams.

Although temperature-dependent trends in waste pyrolysis are well established, this study provides new insight through a direct comparison of food waste and digestate under identical operating conditions, integrating gas-phase composition with detailed char characterisation. By reporting hydrogen production both as volumetric concentration and as mass-normalised yield, the work clarifies the realistic role of pyrolysis relative to hydrogen-oriented thermochemical routes. The results demonstrate that pyrolysis primarily acts as a syngas-forming and feedstock-conditioning step, rather than a hydrogen-maximising process, complementing gasification and catalytic reforming pathways designed to enhance hydrogen recovery. Although the hydrogen volume fraction obtained from the pyrolysis process remains below the threshold required for direct use as high-purity hydrogen, the produced gas mixture constitutes a hydrogen-rich syngas that can be effectively upgraded using established separation and purification technologies. Downstream hydrogen recovery could be achieved through pressure swing adsorption (PSA), membrane-based separation (polymeric or palladium-based), or hybrid systems, depending on the desired purity, recovery rate, and process scale.

Future research should further investigate the long-term stability and functional performance of both food-waste and digestate-derived biochar under application-specific operating environments. Evaluating their behaviour under thermochemical upgrading routes such as gasification or catalytic reforming would help determine performance limits and reaction pathways associated with defect evolution and mineral interactions. Future work should also focus on optimising hydrogen generation through catalytic enhancement or process coupling scenarios, particularly for FW, which demonstrated the highest H_2 response to temperature. Additional studies should also incorporate surface modification strategies (including activation, mineral doping, or functionalization) to assess improvements in adsorption capacity, catalytic reactivity, or electrochemical properties. Finally, scaling the process to pilot-level continuous pyrolysis systems and integrating techno-economic and environmental assessments will be essential to determine the feasibility, lifecycle benefits, and deployment potential of these waste-derived biochar materials. Such assessments will be particularly relevant for validating the role of pyrolysis-derived hydrogen as a thermochemical bio-hydrogen pathway within circular waste-to-energy frameworks.

CRediT authorship contribution statement

Davide Papurello: Writing – original draft, Methodology, Investigation, Formal analysis, Data curation. **Kutlu Somek:** Writing – original draft. **Yeshui Zhang:** Supervision, Funding acquisition, Conceptualization. **Davide Dionisi:** Resources. **Tian Heng Qin:** Investigation, Data curation. **Tian Wang:** Investigation, Data curation. **Andrea Lanzini:** Funding acquisition.

Declaration of competing interest

The authors declare that they have no known competing financial interests or personal relationships that could have appeared to influence the work reported in this paper.

Acknowledgement

This research was supported by the HYWAY project, funded by the European Union (HyWay:101130009).

Appendix A. Supplementary data

Supplementary data to this article can be found online at https://doi.org/10.1016/j.ijhydene.2026.153906.

Nomenclature

Abbreviation/Symbol	Meaning
°C	Degree Celsius
BC	Biochar
BET	Brunauer–Emmett–Teller Surface Area Analysis
BJH	Barrett-Joyner-Halenda
C	Carbon
CH_4	Methane
CO	Carbon Monoxide
CO_2	Carbon Dioxide
DW	Digestate-Derived Biochar/Digestate Waste
EDS	Energy Dispersive X-ray Spectroscopy
FW	Food Waste Biochar
GC	Gas Chromatography
GC–TCD	Gas Chromatography with Thermal Conductivity Detector
H_2	Hydrogen
H_2/CO	Hydrogen-to-Carbon Monoxide Ratio
HTC	HydroThermal Carbonisation
ID/IG	Ratio of Raman D-band to G-band Intensities (structural disorder index)
kV	Kilovolt (SEM accelerating voltage)
m^2/g	Square meter per gram (surface area unit)
N_2	Nitrogen (carrier gas)
O_2	Oxygen
SEM	Scanning Electron Microscopy
SSA	Specific Surface Area
TCD	Thermal Conductivity Detector (GC component)
TGA	Thermogravimetric Analysis
TPO-DTG	Temperature-Programmed Oxidation - Derivative ThermoGravimetry
WWT	WasteWater Treatment sludge
XRD	X-ray Diffraction

References

[1] Wang Z, Li X, Liu H, Mou J, Khan SJ, Lin CSK, Wang Q. Evaluating energy balance and environmental footprint of sludge management in BRICS countries. Water Res 2024;X 25:100255. https://doi.org/10.1016/J.WROA.2024.100255.

[2] Amicarelli V, Lagioia G, Bux C. Global warming potential of food waste through the life cycle assessment: an analytical review. Environ Impact Assess Rev 2021;91:106677. https://doi.org/10.1016/J.EIAR.2021.106677.

[3] Show KY, Lee DJ, Tay JH, Lin CY, Chang JS. Biohydrogen production: current perspectives and the way forward. Int J Hydrogen Energy 2012;37:15616–31. https://doi.org/10.1016/J.IJHYDENE.2012.04.109.

[4] Papurello D, Tomasi L, Silvestri S, Belcari I, Santarelli M, Smeacetto F, Biasioli F. Biogas trace compound removal with ashes using proton transfer reaction time-of-flight mass spectrometry as innovative detection tool. Fuel Process Technol 2016;145:62–75. https://doi.org/10.1016/J.FUPROC.2016.01.028.

[5] Appels L, Baeyens J, Degrève J, Dewil R. Principles and potential of the anaerobic digestion of waste-activated sludge. Prog Energy Combust Sci 2008;34:755–81. https://doi.org/10.1016/J.PECS.2008.06.002.

[6] Giwa AS, Maurice NJ, Luoyan A, Liu X, Yunlong Y, Hong Z. Advances in sewage sludge application and treatment: process integration of plasma pyrolysis and anaerobic digestion with the resource recovery. Heliyon 2023;9:e19765. https://doi.org/10.1016/J.HELIYON.2023.E19765.

[7] Strong PJ, Laycock B, Mahamud SNS, Jensen PD, Lant PA, Tyson G, Pratt S. The opportunity for high-performance biomaterials from methane. Microorganisms 2016;4:4. https://doi.org/10.3390/MICROORGANISMS4010011. 2016.

[8] Mishra RK, Mohanty K. A review of the next-generation biochar production from waste biomass for material applications. Sci Total Environ 2023;904:167171. https://doi.org/10.1016/J.SCITOTENV.2023.167171.

[9] Bolívar Caballero JJ, Zaini IN, Yang W. Reforming processes for syngas production: a mini-review on the current status, challenges, and prospects for biomass conversion to fuels. Applications in Energy and Combustion Science 2022;10:100064. https://doi.org/10.1016/J.JAECS.2022.100064.

[10] Oh DY, Kim D, Park KY. Comparison of pyrolysis gasification of livestock manure, food wastewater, and their co-digested sludge. Chemosphere 2024;357. https://doi.org/10.1016/j.chemosphere.2024.142007.

[11] Global Hydrogen Review 2024 – analysis - IEA, (n.d.). https://www.iea.org/reports/global-hydrogen-review-2024 (accessed November 27, 2025).

[12] Hadroug S, Khiari B, Jellali S, El-Bassi L, Al-Wardy M, Hamdi W, Jeguirim M. Animal manure derived biochars synthesis, characterization and use for wastewater treatment and in agriculture: a recent review. Sci Total Environ 2025;985. https://doi.org/10.1016/j.scitotenv.2025.179751.

[13] Vandana TU, Tripathy BK, Mishra RK, Sharma A, Mohanty K. A review on waste biomass-derived biochar: production, characterisation, and advanced analytical techniques for pollutants assessment in water and wastewater. Process Saf Environ Prot 2025;201. https://doi.org/10.1016/j.psep.2025.107505.

[14] Saif I, Thakur N, Sharma M, Alalawy AI, Jalalah M, Hassan SHA, Zidan NS, Salama ES. Applications of plant and animal-based biochar: insight into environmental remediation and biofuel production. J Water Proc Eng 2025;71. https://doi.org/10.1016/j.jwpe.2025.107278.

[15] Chen WH, Lin BJ, Lin YY, Chu YS, Ubando AT, Show PL, Ong HC, Chang JS, Ho SH, Culaba AB, Pétrissans A, Pétrissans M. Progress in biomass torrefaction: principles, applications and challenges. Prog Energy Combust Sci 2021;82:100887. https://doi.org/10.1016/J.PECS.2020.100887.

[16] Ganesapillai M, Mehta R, Tiwari A, Sinha A, Bakshi HS, Chellappa V, Drewnowski J. Waste to energy: a review of biochar production with emphasis on mathematical modelling and its applications. Heliyon 2023;9:e14873. https://doi.org/10.1016/j.heliyon.2023.e14873.

[17] Zhou S, Yang X, Tran TK, Shen J, An C. Paving the way for biochar production, supply chain, and applications toward a sustainable future. Cleaner Waste Systems 2025;10. https://doi.org/10.1016/j.clwas.2025.100227.

[18] Mishra R, Shu CM, Gollakota ARK, Pan SY. Unveiling the potential of pyrolysis-gasification for hydrogen-rich syngas production from biomass and plastic waste. Energy Convers Manag 2024;321:118997. https://doi.org/10.1016/J.ENCONMAN.2024.118997.

[19] Gao N, Wang X, Li A, Wu C, Yin Z. Hydrogen production from catalytic steam reforming of benzene as tar model compound of biomass gasification. Fuel Process Technol 2016;148:380–7. https://doi.org/10.1016/J.FUPROC.2016.03.019.

[20] Choi IH, Hwang KR, Lee KY, Lee IG. Catalytic steam reforming of biomass-derived acetic acid over modified Ni/γ-Al2O3 for sustainable hydrogen production. Int J Hydrogen Energy 2019;44:180–90. https://doi.org/10.1016/J.IJHYDENE.2018.04.192.

[21] Bartoli M, Pirri CF, Bocchini S, Bartoli M, Pirri CF, Bocchini S. A comprehensive review on hydrogen production from biomass gasification. Molecules 2026;31(31):99. https://doi.org/10.3390/MOLECULES31010099. 2025.

[22] Ahmed II, Gupta AK. Pyrolysis and gasification of food waste: syngas characteristics and char gasification kinetics. Appl Energy 2010;87:101–8. https://doi.org/10.1016/J.APENERGY.2009.08.032.

[23] Raizada A, Yadav S, Tripathi M, Misra S, Mohanty P. Food waste treatment using in situ gasification after pyrolysis to produce hydrogen-rich syngas. Biomass Convers

Biorefinery 2023;13:9689–99. https://doi.org/10.1007/S13399-021-01857-4/FIGURES/7.
[24] Elkhalifa S, Al-Ansari T, Mackey HR, McKay G. Food waste to biochars through pyrolysis: a review. Resour Conserv Recycl 2019;144:310–20. https://doi.org/10.1016/J.RESCONREC.2019.01.024.
[25] Raček J, Chorazy T, Miino MC, Vršanská M, Brtnický M, Mravcová L, Kučerík J, Hlavínek P. Biochar production from the pyrolysis of food waste: characterization and implications for its use. Sustain Chem Pharm 2024;37:101387. https://doi.org/10.1016/J.SCP.2023.101387.
[26] Basinas P, Rusín J, Chamrádová K, Kaldis SP. Pyrolysis of the anaerobic digestion solid by-product: characterization of digestate decomposition and screening of the biochar use as soil amendment and as additive in anaerobic digestion. Energy Convers Manag 2023;277:116658. https://doi.org/10.1016/J.ENCONMAN.2023.116658.
[27] Shivaprasad KV, Heslop J, Roy D, Malik A, Wang Y, Roskilly AP, Bao H. Hydrogen rich syngas production through sewage sludge pyrolysis: a comprehensive experimental investigation and performance optimisation using statistical analysis. Process Saf Environ Prot 2024;187:270–8. https://doi.org/10.1016/J.PSEP.2024.04.071.
[28] Wang F, Wang J, Yu Z, Ma J, Liu L, Wang T, Guo H. Obtaining high yield hydrogen from sewage sludge by two-stage gasification: alkaline pyrolysis coupled with catalytic reforming. ACS Omega 2022;7:22192–8. https://doi.org/10.1021/ACSOMEGA.2C00345/ASSET/IMAGES/LARGE/AO2C00345_0012.JPEG.
[29] Zhang Z, Anjum T, Wang Y, Meng Y, Qin T, Zhang YS, Zhang Y, Li A, Ji G. Hydrogen production from biomass waste gasification under the enhancement of catalyst-sorbent hybrid functional material synthesized from steel slag. Chin J Chem Eng 2025;88:108–23. https://doi.org/10.1016/J.CJCHE.2025.05.041.
[30] Boakye P, Nuagah MB, Oduro-Kwarteng S, Appiah-Effah E, Kanjua J, Antwi AB, Darkwah L, Sarkodie K, Sokama-Neuyam YA. Pyrolysis of municipal food waste: a sustainable potential approach for solid food waste management and organic crop fertilizer production. Sustainable Environment 2023;9. https://doi.org/10.1080/27658511.2023.2260057.
[31] Zhang L, Yao Z, Zhao L, Yu F, Li Z, Yi W, Fu P, Jia J, Zhao Y. Effects of various pyrolysis temperatures on the physicochemical characteristics of crop straw-derived biochars and their application in tar reforming. Catal Today 2024;433. https://doi.org/10.1016/j.cattod.2024.114663.
[32] Sieradzka M, Szkadłubowicz K, Śliz M, Kalemba-Rec I, Kornaus K, Kozinski J, Wilk M. Hydrogen-rich syngas production from sewage sludge and hydrochars via catalytic gasification with SrO. Int J Hydrogen Energy 2025;144:1358–66. https://doi.org/10.1016/j.ijhydene.2025.03.421.
[33] Singh D, Sirini P, Lombardi L. Review of reforming processes for the production of green hydrogen from landfill gas. Energies 2025;18. https://doi.org/10.3390/en18010015.
[34] Akbarzadeh O, Zabidi NAM, Wang G, Kordijazi A, Sadabadi H, Moosavi S, Babadi AA, Hamizi NA, Wahab YA, Ab Rahman M, Sagadevan S, Chowdhury ZZ, Johan MR. Effect of pressure, H2/CO ratio and reduction conditions on Co-Mn/CNT bimetallic catalyst performance in Fischer-Tropsch reaction. Symmetry Plus 2020;12. https://doi.org/10.3390/SYM12050698.
[35] Abou Rjeily M, Cazier F, Randrianalisoa JH, Gennequin C. Detailed analysis of gas, char and bio-oil products of oak wood. Waste Biomass Valoriz 2023;14:325–43. https://doi.org/10.1007/s12649-022-01848-0. [Accessed 15 November 2025].
[36] Ali BI, Gunjo DG. Performance evaluation of throated downdraft gasifier using peanut shell and mango seed hull as a feedstock. Results Eng 2023;20. https://doi.org/10.1016/j.rineng.2023.101642.
[37] Sun K, Wang Y, Zhang L, Shao Y, Li C, Zhang S, Hu X. High yield of carbonaceous material from biomass via pyrolysis-condensation. Chem Eng J 2024;485:149823. https://doi.org/10.1016/J.CEJ.2024.149823.
[38] Sun Y, Gao B, Yao Y, Fang J, Zhang M, Zhou Y, Chen H, Yang L. Effects of feedstock type, production method, and pyrolysis temperature on biochar and hydrochar properties. Chem Eng J 2014;240:574–8. https://doi.org/10.1016/J.CEJ.2013.10.081.
[39] Li F, Cao X, Zhao L, Wang J, Ding Z. Effects of mineral additives on biochar formation: carbon retention, stability, and properties. Environ Sci Technol 2014;48:11211–7. https://doi.org/10.1021/ES501885N/ASSET/IMAGES/LARGE/ES-2014-01885N_0003.JPEG.
[40] Chatterjee R, Sajjadi B, Chen WY, Mattern DL, Hammer N, Raman V, Dorris A. Effect of pyrolysis temperature on PhysicoChemical properties and acoustic-based amination of biochar for efficient CO2 adsorption. Front Energy Res 2020;8:530643. https://doi.org/10.3389/FENRG.2020.00085/BIBTEX.
[41] Vyas A, Chellappa T, Goldfarb JL. Porosity development and reactivity changes of coal–biomass blends during co-pyrolysis at various temperatures. J Anal Appl Pyrolysis 2017;124:79–88. https://doi.org/10.1016/j.jaap.2017.02.018.
[42] Hossain MZ, Bahar MM, Sarkar B, Donne SW, Ok YS, Palansooriya KN, Kirkham MB, Chowdhury S, Bolan N. Biochar and its importance on nutrient dynamics in soil and plant. Biochar 2020;2:379–420. https://doi.org/10.1007/s42773-020-00065-z.
[43] Zhang L, Yao Z, Zhao L, Yu F, Li Z, Yi W, Fu P, Jia J, Zhao Y. Effects of various pyrolysis temperatures on the physicochemical characteristics of crop straw-derived biochars and their application in tar reforming. Catal Today 2024;433:114663. https://doi.org/10.1016/J.CATTOD.2024.114663.
[44] Sudarsan JS, Goel M, Jahangiri H, Rout PR, Tavakolian M, Briggs C, Haynes-Parry M, Asthana A, Lakshmipathy R, Prabhu SV, Nithiyanantham S. Sustainable food waste management: a critical review on biochar production and applications. Sustainable Food Technology 2025. https://doi.org/10.1039/d5fb00087d.
[45] Jagadeesh N, Sundaram B. Adsorption of pollutants from wastewater by biochar: a review. J Hazard Mater Adv 2023;9. https://doi.org/10.1016/j.hazadv.2022.100226.
[46] Clemente JS, Beauchemin S, Thibault Y, Mackinnon T, Smith D. Differentiating inorganics in biochars produced at commercial scale using principal component analysis. ACS Omega 2018;3:6931–44. https://doi.org/10.1021/acsomega.8b00523.
[47] Sahoo SS, Vijay VK, Chandra R, Kumar H. Production and characterization of biochar produced from slow pyrolysis of pigeon pea stalk and bamboo. Clean Eng Technol 2021;3:100101. https://doi.org/10.1016/J.CLET.2021.100101.
[48] Pradhan S, Parthasarathy P, Mackey HR, Al-Ansari T, McKay G. Food waste biochar: a sustainable solution for agriculture application and soil–water remediation. Carbon Res 2024;3. https://doi.org/10.1007/s44246-024-00123-2.
[49] Fu P, Yi W, Bai X, Li Z, Hu S, Xiang J. Effect of temperature on gas composition and char structural features of pyrolyzed agricultural residues. Bioresour Technol 2011;102:8211–9. https://doi.org/10.1016/j.biortech.2011.05.083.